ACS APPLIED MATERIALS & INTERFACES

www.acsami.org

Research Article

Polymerization-Achieved Cyclodextrin Slide-Ring Supramolecular Hydrogel Self-Generating Flexible Electronic Device

Xiaoyong Yu, Wenjin An, Linnan Jiang, Wenwen Xu, Zhenkai Qian, Lihua Wang, Yong Chen,* and Yu Liu*

Cite This: *ACS Appl. Mater. Interfaces* 2024, 16, 68229−68236

Read Online

ACCESS | Metrics & More | Article Recommendations | Supporting Information

ABSTRACT: Supramolecular flexible electronic devices are one of the research hotspots due to their application in the fields of chemistry, biology, and materials. Herein, we reported a slide-ring supramolecular flexible electronic device, which is constructed by acrylamide (AAm), acrylic acid (AA), carboxymethyl-α-cyclodextrin (CM-α-CD), PEG_{20000} diacrylate ($PEG_{20000}DA$), and calcium chloride via the photoinitiated polymerization, displaying not only the mechanical force-responded self-generation but also the human−computer information transfer. As compared with the polymer hydrogel, the addition of α-CD polypseudorotaxane to the hydrogel has notably enhanced both the tensile length and the tensile toughness, making it more suitable for flexible electronic device applications. The hydrogel can be stretched to ca. 15 times its original length and quickly recovers after the external force is removed. In addition, it also exhibits a conductivity of 0.21 S/m, demonstrating good electrical conductivity. Significantly, based on the slide-ring supramolecular array for energy harvesting, it can generate an open-circuit voltage of 420 V using the contact separation method for testing, which can be used as a flexible electronic device for human−computer information transfer.

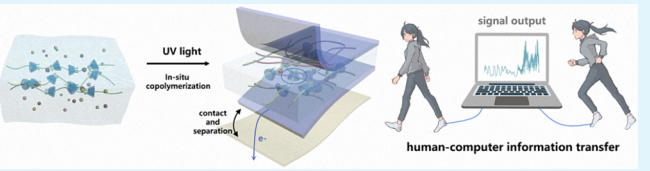

KEYWORDS: *slide-ring hydrogel, cyclodextrin, supramolecular, polypseudorotaxane, flexible electronic device*

INTRODUCTION

The supramolecular slide-ring material has garnered widespread attention due to its excellent ability on the enhancement of polymer flexibility,[1−4] self-recovery,[5−7] and fatigue resistance,[8,9] and it is widely used to construct novel macromolecular materials.[10−13] During the research progress of the slide-ring material, being mainly macrocyclic, the cyclodextrin hydrophobic cavities can encapsulate guest molecules for in situ polymerization or slide along the polymer chains to form flexible slide-ring materials.[14−19] Possessing the sliding rings on the polymer chain, the hydrogel can be responsible for stress, therefore improving the mechanical properties of hydrogels. Recently, Ito et al. reported the slide-ring hydrogel with a polyethylene glycol chain as the "line" and hydroxypropyl-α-cyclodextrin as the "slide ring".[20] When the coverage rate of cyclodextrin on the polyethylene glycol chain was controlled at 2%, the hydrogel exhibited toughness similar to the natural rubber. Bao et al. introduced the polyrotaxane constructed from a polyethylene glycol backbone and sliding cyclodextrins functionalized with PEG methacrylate side chains as a supramolecular cross-linker into the PEDOT:PSS system.[21] The formation of the supramolecular topological network effectively induced high conductivity, stretchability, and photopatternability. Additionally, the work was further applied to the collection of electromyography signals from the octopus and the precise localized neural modulation of the rat brainstem. Ke et al. reported a novel strategy for constructing rotaxanes based on γ-cyclodextrin.[22] The slide-ring cross-linkers were prepared by forming a double-threaded structure between γ-cyclodextrin and telechelic PEG, effectively improving the mechanical properties of the hydrogels to achieve both high elasticity and high toughness. In addition, high-performance slide-ring stress sensors exhibiting high sensitivity and a wide detection range were constructed using 3D printing. Liu et al. reported the polypseudorotaxane constructed by hydroxypropyl-α-cyclodextrin and acrylamide-PEG_{20000}-acrylamide, followed by in situ polymerization of rotaxane and acrylamide via photopolymerization.[23] When using 1,4-butanediol diglycidyl ether to cross-link the cyclodextrin rings and adding calcium ions to enhance the ionic conductivity, the obtained hydrogel showed good mechanical properties and can be used in wearable strain sensors for real-time monitoring of human motion signals. Although slide-ring hydrogels have been applied in various fields,[24−28] their use to enhance the mechanical performance of flexible electronic devices in self-generating human−computer information

Received: August 2, 2024
Revised: November 13, 2024
Accepted: November 19, 2024
Published: November 27, 2024

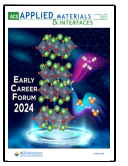

https://doi.org/10.1021/acsami.4c12962
ACS Appl. Mater. Interfaces 2024, 16, 68229−68236

Scheme 1. Construction of CM-α-CD/PEG$_{20000}$DA/AAM/AA Hydrogel and the Demonstration of Sandwich-Shaped TENG with Motion Sensing

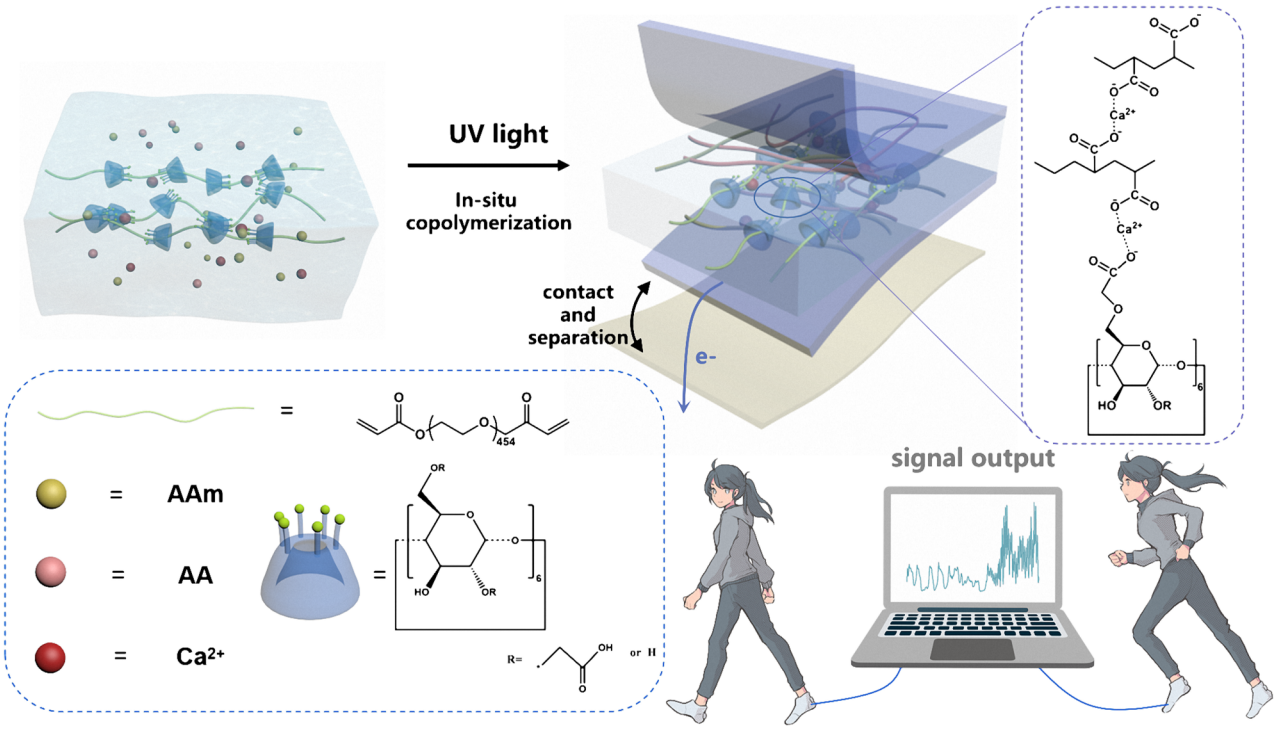

transfer systems has been rarely reported to the best of our knowledge.[29−33]

Herein, we reported a self-generating supramolecular slide-ring hydrogel material prepared by photoinitiated polymerization of an acrylamide + acrylic acid + calcium chloride mixture with the polypseudorotaxane cross-linker constructed from PEG$_{20000}$ diacrylate (PEG$_{20000}$DA) and carboxymethyl-α-cyclodextrin (CM-α-CD) sliding along the chain (Scheme 1). In this system, acrylamide and acrylic acid served as monomers, while rotaxane formed by PEG and carboxymethyl-α-cyclodextrin acted as a cross-linker. I_{2959} was used as a photoinitiator for UV polymerization, and calcium ions were added to enhance conductivity. The main reason for calcium ion conductivity could be that Ca^{2+} particles are charged particles that can move freely in the solution. When an electric field is applied, the charged ions migrate toward the electrodes. The movement of ions allows the hydrogel to conduct electricity. Compared to the polymer hydrogel, incorporating α-CD polypseudorotaxane into the hydrogel significantly improved both the tensile length and tensile toughness, making it more ideal for flexible electronic device applications. The slide-ring structure plays a crucial role in enhancing the mechanical properties of hydrogel. The slide-ring hydrogel with excellent mechanical properties and electrical conductivity was applied to the flexible electrodes of the triboelectric nanogenerator (TENG) to adapt to the deformation loss. As a promising flexible electronic device, it not only enables energy harvesting but also demonstrates excellent human−computer information transfer capabilities under different motion (walking, running) modes and sites (finger, wrist, elbow, knee movements).

RESULTS AND DISCUSSION

CM-α-CD and PEG$_{20000}$DA, either of which can be synthesized through a one-step reaction, were assembled to a polypseudorotaxane structure via host−guest interactions in aqueous solution (Figures S1−S3). The 2D ROESY experiment visually illustrated the formation of a rotaxane structure. The signal of interior H-3/H-5 protons of CM-α-CD at 4.00−3.75 ppm showed obvious NOE correlations with the signal of −OCH2− protons of PEG at 3.69 ppm, indicating that the PEG chain was threaded into the cavity of CM-α-CD (Figure S4). Subsequently, a polypseudorotaxane aqueous solution was added to the mixed solution of acrylic acid and acrylamide containing a small amount of photoinitiator I_{2959}. After the addition of Ca^{2+} to cross-link the acrylic acid and CM-α-CD, the solution was polymerized under ultraviolet light of 365 nm to form the hydrogel in a white translucent state. In this hydrogel, the copolymerization of acrylamide and acrylic acid with polypseudorotaxane formed a three-dimensional network structure, and the polypseudorotaxane was terminated by the newly formed polyacrylamide-acrylic acid chain. The coordination bond between calcium ion and carboxyl group formed another cross-linking network, providing the hydrogel a dual-cross-linking structure.[34] Simultaneously, the cross-linking between calcium ions and carboxyl groups breaks prior to the covalent bond network under external forces, thus effectively dissipating the mechanical energy and enhancing the toughness of the material. Due to the existence of cross-linking bonds and hydrogen bonds, the hydrogel exhibited a certain self-healing ability. Since the slide-ring hydrogel is formed through the copolymerization of polypseudorotaxane, acrylamide, and acrylic acid, it is difficult to measure the amount of free cyclodextrins. However, the free CM-α-CD can coordinate with calcium ions, further enhancing the mechanical properties of the hydrogel. In a control experiment, we also

https://doi.org/10.1021/acsami.4c12962
ACS Appl. Mater. Interfaces 2024, 16, 68229−68236

prepared acrylamide hydrogels with polypseudorotaxane and calcium ions, and cross-linking was only observed among CM-α-CDs.

The CM-α-CD/PEG_{20000}DA/AAM/AA hydrogel (CPAA hydrogel) and CM-α-CD/PEG_{20000}DA/AAM hydrogel (CP hydrogel) were lyophilized and then tested by SEM (Figures 1a,b). SEM images of both hydrogels revealed distinct three-dimensional porous network structures, with the pore sizes of the CPAA hydrogel smaller than those of the CP hydrogel, indicating the formation of a denser cross-linking network structure in the CPAA hydrogel. The EDS analysis of the CP hydrogel and CPAA hydrogel clearly showed the presence and distribution of calcium ions, sodium ions, and chloride ions within the hydrogel (Figures S5 and S6). The FTIR spectra of the lyophilized CP hydrogel and CPAA hydrogel (Figure S7) showed the characteristic peaks of amide at 3361, 3189, 1661, and 1623 cm^{-1}. Among them, the characteristic peaks at 3361 and 3189 cm^{-1} were assigned to the N−H stretching vibration, the characteristic peak at 1661 cm^{-1} was assigned to the C═O stretching vibration, and the characteristic peak at 1623 cm^{-1} was assigned to the N−H bending vibration. In addition, the peak at 1428 cm^{-1} was assigned to the asymmetric and symmetrical stretching vibrations of COO− in the carboxyl group. The thermogravimetric test of the CPAA hydrogel after drying was conducted (Figure 1c), where the hydrogel showed good thermal stability below 200 °C. By comparing the weight of the hydrogel before and after drying, the water content of the hydrogel was calculated to be 62.9%. To further verify the conductivity of the hydrogel, the resistance was measured by electrochemical impedance spectroscopy, and its conductivity was subsequently calculated to be 0.21 S/m. These results indicated that the hydrogel possessed good electrical conductivity, meeting the requirements for the TENG electrodes (Figure S8).

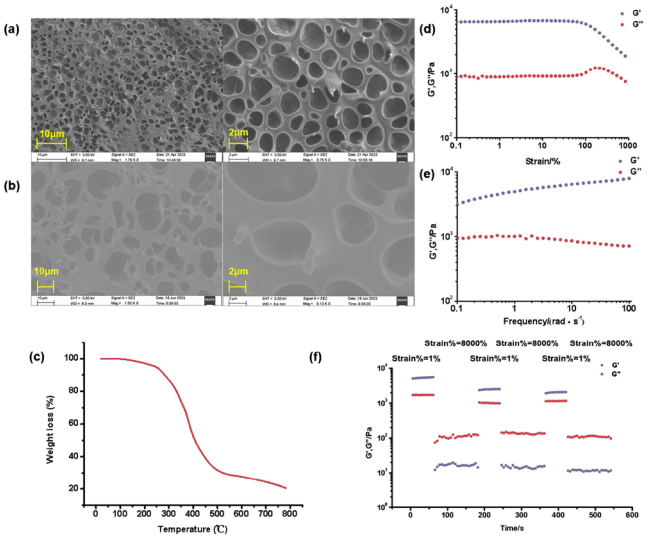

Figure 1. (a) SEM image of frozen-dried CM-α-CD/PEG_{20000}DA/AAM/AA hydrogel. (b) SEM image of frozen-dried CM-α-CD/PEG_{20000}DA/AAM hydrogel. (c) TGA curve of the CM-α-CD/PEG_{20000}DA/AAM/AA hydrogel. (d) G' (storage modulus) and G'' (loss modulus) as functions of strain. (e) G' and G'' as functions of frequency. (f) Alternate step strain sweep (rheological self-healing test) with the fixed frequency of 1 Hz. Amplitude oscillatory strain levels of hydrogel were turned between 1 and 8000% (CM-α-CD/PEG_{20000}DA/AAM/AA hydrogel, PEG:CM-α-CD = 1:5).

The rheological tests of CPAA hydrogel and CP hydrogel with various rotaxane contents were conducted to investigate the mechanical properties of slide-ring supramolecular hydrogels (Figure 1d,e and Figures S9−S11). In the stress scanning curves of both these hydrogels, as the stress increased from 0.1 to 1000%, the storage elastic modulus (G') was first greater than the loss elastic modulus (G'') and then gradually tended to intersect, indicating the gradual destruction of hydrogel with the increase of stress. In the frequency scanning curve, as frequency increased from 1 to 100%, both G' and G'' gradually increased and remained parallel, while G' was consistently larger than G'', indicating that the hydrogel maintained a stable state within this range. Notably, the difference in rotaxane contents had no obvious effect on the rheological properties of hydrogels. However, the storage modulus of the CPAA hydrogel was significantly higher than that of the CP hydrogel, confirming that the coordination cross-linking of calcium ions and carboxyl groups enhances the mechanical property of the hydrogel. Subsequently, the rheology of the CPAA hydrogel was tested at a fixed frequency of 1 Hz with stepwise strain (strain = 8000−1−8000−1%) at 25 °C to evaluate its self-healing performance (Figure 1f). At a strain of 8000%, the hydrogel was destroyed and lost its mechanical strength ($G'' > G'$). Upon the reduction of strain to 1%, the reversible nature of the coordination bond and hydrogen bond facilitated the healing of the hydrogel network from the previously disrupted sol state, leading to the rapid recovery of mechanical strength ($G' > G''$). The self-healing properties mainly contribute to the coordination with the slide-ring structure and Ca^{2+}, leading to the reversible transformation between sol and hydrogel. The self-healing efficiency is quantified based on the ratio of the storage modulus before and after healing, and the efficiency is calculated as 46.3%. These results confirmed the self-healing property of the CPAA hydrogel network.

CP hydrogel and CPAA hydrogel with varying rotaxane contents underwent tensile testing to assess their mechanical properties, while tensile testing of the CP hydrogel without the influence of a metal coordination bond was carried out to demonstrate the effective enhancement of hydrogel mechanical properties, with the addition of slide-ring structures. It was observed that with increasing rotaxane content, the tensile fracture length and the tensile toughness of the hydrogel increased as the PEG:CM-α-CD ratio ranged from 1:0 to 1:10, the tensile fracture length increased from 1285 to 1488% (Figure S12), and the tensile toughness and the elastic modulus also increased accordingly (Figure S13). The presence of the rotaxane structure enabled the slide ring on the chain to disperse the stress throughout the entire hydrogel, thereby enhancing its stretching ability. However, due to the low content of carboxyl groups in hydrogels, the cross-linking with calcium ions was insufficient, and many rings were not cross-linked and fixed. Therefore, it was speculated that adding acrylic acid to increase the cross-linking site would further enhance the effect of rotaxane on the hydrogels. The fatigue resistance of CP hydrogel with a ratio of PEG: CM-α-CD of 1:5 was tested (Figure S14). The area of hysteresis loop was large in the first stretching cycle, but in the subsequent cycles, the hydrogel could almost recover completely and the area of hysteresis loop was also greatly reduced almost without hysteresis lag. This phenomenon was attributed to the presence of a small amount of unpolymerized polypseudorotaxane in the hydrogel, which formed an unstable structure irreversibly destroyed in the first cycle. Additionally, the cyclic

https://doi.org/10.1021/acsami.4c12962
ACS Appl. Mater. Interfaces 2024, 16, 68229−68236

residue strain testing was conducted by subjecting the hydrogel to 10 cycles under a strain of 500%. The residue strain was 7.95% after the first cycle, which remained basically unchanged in the subsequent cycles and finally did not exceed 9% after 10 cycles (Figure S15).

The tensile test of the CPAA hydrogel with adding acrylic acid was also performed, revealing that the hydrogel can be stretched to >10 times its own length without fracturing (Figure S16). Compared to the CP hydrogel, the CPAA hydrogel exhibited significantly increased strength and tensile toughness, but the tensile fracture length decreased due to the increase of hydrogel plasticity caused by the elevated levels of carboxyl group and calcium ion coordination. When the ratio of PEG:CM-α-CD increased to 1:5, the strength of the hydrogel increased, and the fracture length of the hydrogel also significantly increased from 1078 to 1383% (Figure 2a),

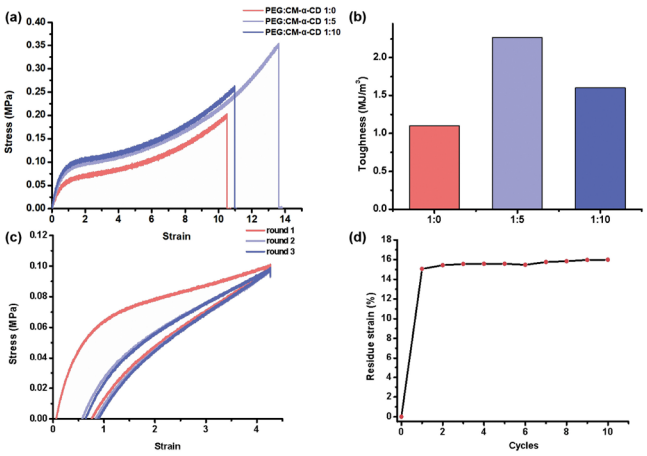

Figure 2. (a) Tensile stress−strain curves of CM-α-CD/PEG_{20000}DA/AAM/AA hydrogels with different polypseudorotaxane components (red, PEG:CM-α-CD = 1:0; light blue, PEG:CM-α-CD = 1:5; dark blue, PEG:CM-α-CD = 1:10). (b) Tensile toughness of hydrogel with the PEG_{20000}:CM-α-CD ratios of 1:0, 1:5, and 1:10. (c) Tensile loading−unloading curves of CM-α-CD/PEG_{20000}DA/AAM/AA hydrogels with PEG:CM-α-CD = 1:5. (d) Residue strain as a function of cycle times at a strain of 500% (PEG:CM-α-CD = 1:5).

accompanied by the increased tensile toughness from 1.10 to 2.27 MJ/m^3 (Figure 2b) and the fracture energy from 19.56 to 58.8 kJ/m^2 (Figure S17). That is, the addition of rotaxane to CPAA hydrogel had a better effect on the mechanical properties of the hydrogel, particularly increasing the tensile fracture length due to the more extensive cross-linking of slide rings on the chain, effectively avoiding the increase of hydrogel brittleness. Moreover, the addition of acrylic acid also increased the number of coordination bonds and thus strengthened the mechanical properties of the hydrogel. When further increasing the ratio of PEG:CM-α-CD to 1:10, the tensile fracture length slightly decreased to 1119% and the tensile toughness dropped to 1.60 MJ/m^3, but the elastic modulus increased significantly (Figure S18). This may be due to the presence of excessive CM-α-CDs on the polyethylene glycol chains, whose accumulation narrows the sliding range of individual cyclodextrin and thus increases the hydrogel brittleness. Considering that the CPAA hydrogel with a PEG:CM-α-CD ratio of 1:5 exhibited the best mechanical properties, it was chosen for the antifatigue test (Figure 2c). The cyclic residue strain of the hydrogel was also tested by 10 cycles under 500% strain. After the first cycle, the residue strain was 15.05%, which was higher than that of the CP hydrogel and then remained basically unchanged in subsequent cycles (Figure 2d). Through further fatigue threshold experiments, it can be observed that the fatigue threshold of the CPAA hydrogel with a ratio of 1:5 increased from 0.124 to 0.331 kJ/m^2 compared to the CPAA hydrogel with a ratio of 1:0. This demonstrated that the addition of the rotaxane effectively enhanced the fatigue resistance of the hydrogel (Figure S19).

As the ratio of PEG:CM-α-CD increased from 1:0 to 1:10, the compressive strength of the CPAA hydrogel increased from 127.68 to 166.75 kPa, demonstrating the good resilience of hydrogel (Figure S20a). Additionally, cyclic compression also showed that the sample can approach the nondestructive recovery from the second compression cycles (Figure S20b). Subsequently, the CPAA hydrogel was applied to the flexible electrode of the TENG with the single-electrode mode, where the CPAA hydrogel electrode was sandwiched between two layers of polydimethylsiloxane (PDMS) Sylgard 184 film for encapsulation. A stretchable single-electrode TENG with a three-layer structure was constructed by connecting the CPAA hydrogel electrode with copper foil tape and copper wire. In the TENG device, the slide-ring supramolecular array cross-linking with Ca^{2+} is responsible for energy harvesting, therefore providing the flexible hydrogel electrodes' energy-harvesting ability. The hydrogel remained stable in the air for at least 1 day without visible hardening and bending but was basically unchanged in PDMS or 3 M VHB 4905, indicating that the encapsulation effectively maintained the stability of hydrogels and prevented the water loss from the hydrogel. Two different dielectric materials, VHB tape and latex sheets cut from latex gloves, which are more inclined to lose electrons and therefore have more frictional positivity, were selected for testing with PDMS that has more frictional negativity.

The single-electrode TENG performance of the CPAA hydrogel was evaluated using the contact separation method, where the hydrogel was encapsulated by PDMS and VHB was selected as another dielectric material. To evaluate the energy-harvesting capability of the TENG, the effects of different contact frequencies on the electrical output were also investigated. During the test, the output voltage of the TENG remained nearly unchanged with only slight fluctuation over multiple cycles (Figure S21). When the frequency of contact separation changed to 0.67, 1 and 1.4 Hz, the open-circuit voltage (*Voc*) and the short-circuit charge quantity (Qsc) values remained as 420 V and 6.0 nC, respectively, while the short-circuit current (Isc) increased from 0.19 to 0.4 μA with increasing frequency (Figure 3), demonstrating good power generation performance. When replacing VHB with latex as another dielectric material, Voc, Qsc, and Isc were measured as 355 V, 5.0 nC, and 0.28 μA, respectively, at 1 Hz (Figure S22). Similarly, when the encapsulation material of the hydrogel was changed to VHB and the latex was selected as another dielectric material to assemble the TENG, Voc, Qsc, and Isc were tested as 175 V, 4.3 nC, and 0.08 μA, respectively, at 1 Hz (Figure S23). Compared with that of the PDMS/VHB pair, the difference in electron acquisition and loss ability of PDMS/latex was smaller, while those of the VHB/latex pair were the smallest. Consequently, less charge generated at the interface, resulting in a decrease of voltage.

Accordingly, a proposed sensor was prepared using the single-electrode TENG, with PDMS and nitrile gloves chosen as the dielectric materials. When wearing nitrile gloves to press

https://doi.org/10.1021/acsami.4c12962
ACS Appl. Mater. Interfaces 2024, 16, 68229−68236

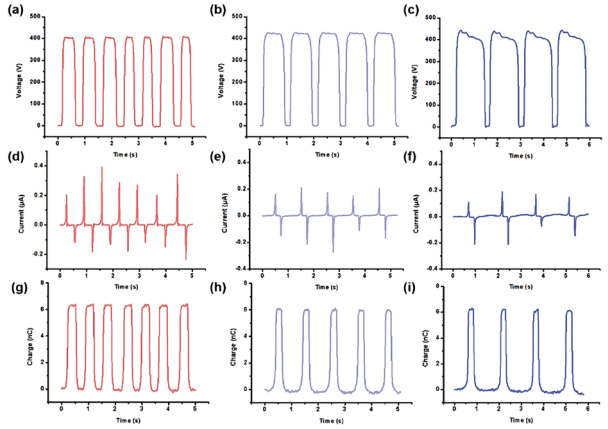

Figure 3. (a) Voc, (d) Isc, and (g) Qsc of a PDMS-VHB single-electrode TENG with a contact separation frequency of 1.4 Hz. (b) Voc, (e) Isc, and (h) Qsc of a PDMS-VHB single-electrode TENG with a contact separation frequency of 1 Hz. (c) Voc, (f) Isc, and (i) Qsc of a PDMS-VHB single-electrode TENG with a contact separation frequency of 0.67 Hz.

the hydrogel encapsulated with PDMS, an obvious electrical signal was generated during the pressing process. Different electrical signals were observed when applying larger or smaller pressure to the sensor quickly or slowly, reflecting the force and speed of the pressing (Figure 4 and Supplementary Movie 1). When pressing the TENG with larger pressure, a higher electrical signal was obtained, whereas when pressing with smaller pressure, it led to the lower electrical signal. Additionally, pressing the TENG quickly resulted in a higher frequency of the electrical signal, while pressing slowly led to a slower frequency. Therefore, the sensors based on the TENG can effectively reflect the force and speed of pressing so that it can be applied to pressure sensing applications.

In addition to pressure sensing, attaching the stretchable TENG to the different body sites (finger, wrist, elbow, and knee) served as a sensor for monitoring human motion (Figure 5a, Figure S24, and Supplementary Movie 2). For example, as the fingers or wrists bent and straightened, the contact area between the PDMS layer and the glove worn on the hand changed, resulting in significant variations in the voltage output. The monitored voltage changes increased with the amplitude of the motion. Therefore, the motion sensor detected the bending angles of fingers or wrists by analyzing the changes in the output voltage, thereby monitoring the frequency of the movement. Similarly, by attaching the TENG to the skin at the elbow and knee, the range and frequency of elbow and knee movements can be monitored. Moreover, due to the excellent mechanical properties of the hydrogel, the TENG was applied in high-pressure applications, such as harvesting mechanical energy during walking and running (Figure 5b). The TENG encapsulated with VHB was assembled on the soles of shoes to detect walking/running motion. Compared to walking, running generated the higher frequency and pressure to the soles, resulting in an increase in generated voltage from ~50 to ~200 V, indicating that the TENG can effectively monitor the human motion state. Notably, the hydrogel did not rupture after testing, demonstrating its stability under high-pressure applications. To further explore the energy harvesting capability of TENG, the equivalent circuit of a self-charging system was constructed. The alternating current generated by the TENG was converted to direct current through a rectifier to charge commercial capacitors. The 1 and 4.7 μF capacitors were charged at a contact separation frequency of 1 Hz. By detection of the voltage increase across the capacitors, it was confirmed that the

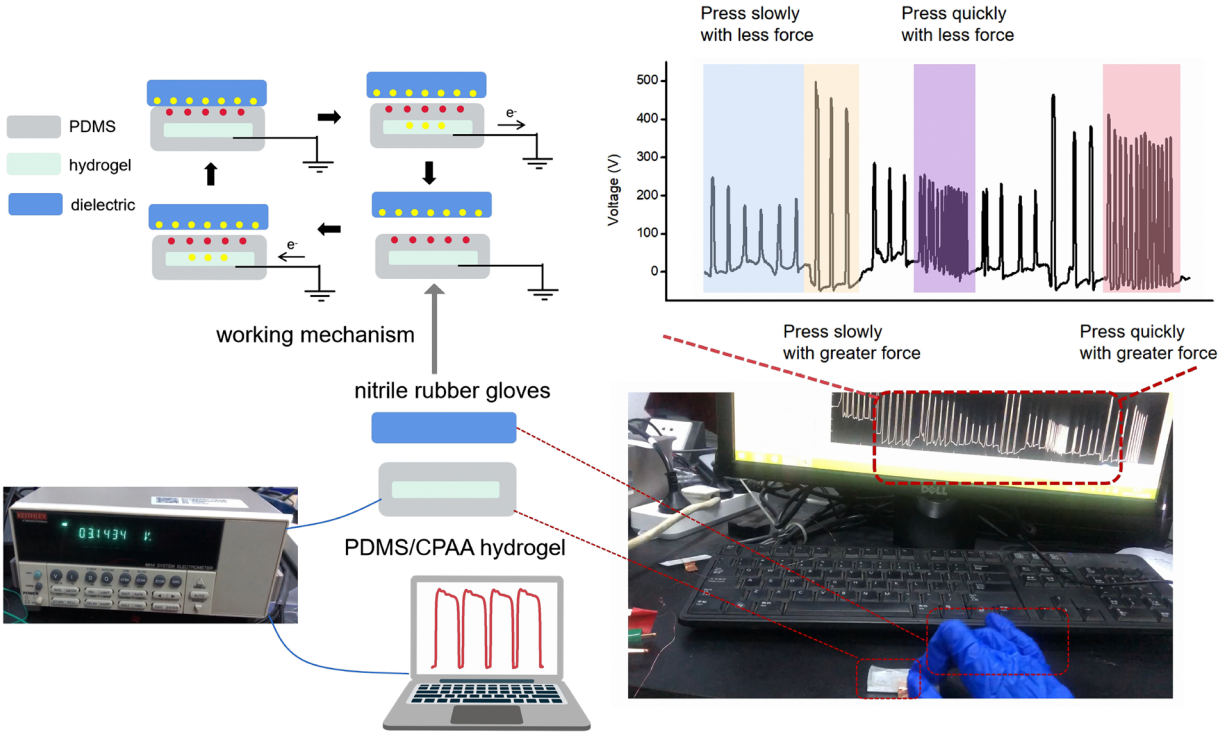

Figure 4. Scheme of the working mechanism of the single-electrode hydrogel TENG and the electrical signal of sensor based on the single-electrode TENG pressed with different force and frequency.

https://doi.org/10.1021/acsami.4c12962
ACS Appl. Mater. Interfaces 2024, 16, 68229−68236

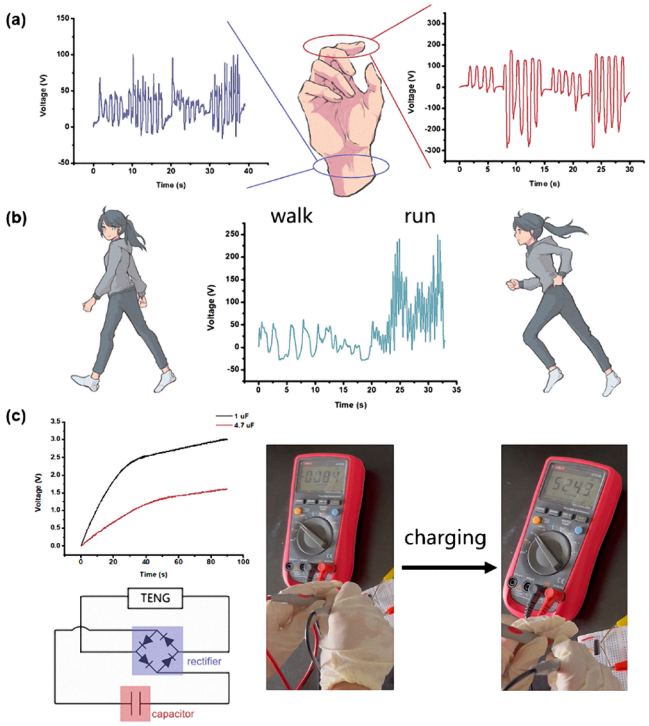

Figure 5. (a) Schematic of the active motion sensor installed on the finger and wrist for monitoring the motion state, along with the voltage output of the motion sensor during repeated motion processes. (b) Schematic diagram of the active motion sensor installed on the sole of the shoe for monitoring the motion state to harvest walking and running energy, along with the voltage output of the motion sensor during walking and running processes. (c) Equivalent circuit of the self-charging system utilizing energy obtained from TENG to power capacitors, along with the voltage of 1 and 4.7 μF capacitors charged by TENG with the contact separation frequency of 1 Hz.

TENG successfully harvested and stored energy in the capacitors (Figure 5c and Supplementary Movie 3).

CONCLUSIONS

In summary, we successfully constructed a self-generating slide-ring hydrogel using carboxymethyl-α-cyclodextrin (CM-α-CD), acrylamide (AAm), acrylic acid (AA), PEG_{20000} diacrylate ($PEG_{20000}DA$), and calcium chloride, which can be applied in the human−computer information transfer system. Herein, calcium ions coordinate with the carboxyl groups in AA and CM-α-CD to establish a cross-linking network within the hydrogel, facilitating the formation of a slide-ring supramolecular structure. Experiment results demonstrated that the incorporation of rotaxane effectively enhances the mechanical properties of the hydrogels. When applying this slide-ring hydrogel to the electrode of TENG, the slide-ring hydrogel effectively promotes the generation of 10^2 V-level voltage and μA-level electric current by simply rubbing the hydrogel. Benefiting from the available voltage and current changes of the slide-ring hydrogel corresponding to various human body movements for different sites (finger, wrist, elbow, knee) and modes (walking, running), the slide-ring hydrogel can be used for self-generating flexible information transformation from human skin to computer. We believe that the supramolecular self-generating slide-ring hydrogel based on cyclodextrin provides a fresh perspective for the preparation of flexible electronic device materials.

EXPERIMENTAL SECTION

Materials. Bromoacetic acid, acrylamide (AAm), acrylic acid (AA), and calcium chloride ($CaCl_2$) dehydrate were purchased from Shanghai Aladdin Biochemical Technology Co., Ltd. Polyethylene glycol (PEG_{20000}), acrylamide acryl chloride, and 2-hydroxy-4′-(2-hydroxyethoxy)-2-methyl propiophenone (I_{2959}) were purchased from Tianjin Heowns Biochemical Technology Co., Ltd. α-Cyclodextrin was purchased from Zhiyuan Biotechnology Co., Ltd. Triethylamine (TEA) was purchased from Beijing Bailingwei Technology Co., Ltd., without further purification. PEG_{20000} diacrylate ($PEG_{20000}DA$) was prepared by using reported methods.[8]

Preparation of CM-α-CD/$PEG_{20000}DA$ Polypseudorotaxane. 200 mg of PEG_{20000}-DA was dissolved in 10 mL of deionized water, and then a corresponding ratio of CM-α-CD was added. After an ultrasonic treatment for 30 min, the mixture was refrigerated at 0 °C for 48 h to get the polypseudorotaxane solution.

Preparation of the CM-α-CD/$PEG_{20000}DA$/AAM Hydrogel. 200 μL of well-shaken CM-α-CD/$PEG_{20000}DA$ polypseudorotaxane solution was added to a sample tube with 800 μL of 300 mg/mL acrylamide aqueous solution, and then 1 mg of I_{2959} and 40 mg of calcium chloride were added to the system. After the tube was shaken until the mixture became clear, the mixture was transferred to a Teflon mold, covered with a glass coverslip, and irradiated under UV light (365 nm, using portable UV analyzer ZF-7A) for 15 min to get the CP hydrogel.

Preparation of the CM-α-CD/$PEG_{20000}DA$/AAM/AA Hydrogel. 200 μL of well-shaken CM-α-CD/$PEG_{20000}DA$ polypseudorotaxane solution was added to a sample tube with 600 μL of 300 mg/mL acrylamide aqueous solution and 200 μL of acrylic acid, and then 10 mg of I_{2959} and 40 mg of calcium chloride were added to the system. After the tube was shaken until the mixture became clear, the mixture was transferred to a Teflon mold, covered with a glass coverslip, and irradiated under UV light (365 nm, using portable UV analyzer ZF-7A) for 20 min to get the CPAA hydrogel.

The hydrogel can also be prepared by thermal initiation. 200 μL of well-shaken CM-α-CD/$PEG_{20000}DA$ polypseudorotaxane solution was added to a sample tube with 600 μL of 300 mg/mL acrylamide aqueous solution and 200 μL of acrylic acid, and then 1 mg of $K_2S_2O_8$ and 40 mg of calcium chloride were added to the system. After shaking up the tube until the mixture became clear, the mixture was transferred to a Teflon mold, covered with a glass coverslip, and heated in the oven at 60 °C for two h to get the CPAA hydrogel.

ASSOCIATED CONTENT

Supporting Information

The Supporting Information is available free of charge at https://pubs.acs.org/doi/10.1021/acsami.4c12962.

Working mechanism of the single-electrode hydrogel TENG and the electrical signal of sensor base on the single-electrode TENG pressed with different forces and frequencies (MP4)

Active motion sensor installed on the finger and wrist for monitoring the motion state, along with the voltage output of the motion sensor during repeated motion processes (MP4)

Equivalent circuit of the self-charging system utilizing energy obtained from TENG to power capacitors, along with the voltage of 1 μF capacitor charged by the TENG with the contact separation frequency of 1 Hz (MP4)

Synthesis and characterization of compounds, NMR spectra, 2D ROESY, FTIR spectrum, SEM images, representative EDS spectrum, rheological tests, electrochemical AC impedance spectra, tensile stress−strain

https://doi.org/10.1021/acsami.4c12962
ACS Appl. Mater. Interfaces 2024, 16, 68229−68236

curves, tensile toughness, residue strain, fracture energy, fatigue threshold, Young's modulus, compressive stress−strain curves, open-circuit voltage (Voc), short-circuit charge quantity (Qsc), and short-circuit current (Isc) of the TENG and schematic of the active motion sensor provided (PDF)

AUTHOR INFORMATION

Corresponding Authors

Yong Chen − *College of Chemistry, State Key Laboratory of Elemento-Organic Chemistry, Nankai University, Tianjin 300071, P. R. China*; Email: chenyong@nankai.edu.cn

Yu Liu − *College of Chemistry, State Key Laboratory of Elemento-Organic Chemistry, Nankai University, Tianjin 300071, P. R. China*; orcid.org/0000-0001-8723-1896; Email: yuliu@nankai.edu.cn

Authors

Xiaoyong Yu − *College of Chemistry, State Key Laboratory of Elemento-Organic Chemistry, Nankai University, Tianjin 300071, P. R. China*

Wenjin An − *College of Chemistry, State Key Laboratory of Elemento-Organic Chemistry, Nankai University, Tianjin 300071, P. R. China*

Linnan Jiang − *College of Chemistry, State Key Laboratory of Elemento-Organic Chemistry, Nankai University, Tianjin 300071, P. R. China*

Wenwen Xu − *College of Chemistry, State Key Laboratory of Elemento-Organic Chemistry, Nankai University, Tianjin 300071, P. R. China*

Zhenkai Qian − *College of Chemistry, State Key Laboratory of Elemento-Organic Chemistry, Nankai University, Tianjin 300071, P. R. China*

Lihua Wang − *College of Chemistry, State Key Laboratory of Elemento-Organic Chemistry, Nankai University, Tianjin 300071, P. R. China*

Complete contact information is available at: https://pubs.acs.org/10.1021/acsami.4c12962

Notes

The authors declare no competing financial interest.

ACKNOWLEDGMENTS

This work was financially supported by the National Natural Science Foundation of China (grant 22131008).

REFERENCES

(1) Hashimoto, K.; Shiwaku, T.; Aoki, H.; Yokoyama, H.; Mayumi, K.; Ito, K. Strain-induced crystallization and phase separation used for fabricating a tough and stiff slide-ring solid polymer electrolyte. *Sci. Adv.* **2023**, *9*, No. eadi8505.

(2) Zhang, Y.; Chen, Y.; Zhang, H.; Chen, L.; Bo, Q.; Liu, Y. Slide-Ring Supramolecular Mechanoresponsive Elastomer with Reversible Luminescence Behavior. *Adv. Opt. Mater.* **2023**, *11*, No. 2202828.

(3) Chen, L.; Sheng, X.; Li, G.; Huang, F. Mechanically interlocked polymers based on rotaxanes. *Chem. Soc. Rev.* **2022**, *51*, 7046−7065.

(4) Gavrilov, A. A.; Potemkin, I. I. Adaptive structure of gels and microgels with sliding cross-links: enhanced softness, stretchability and permeability. *Soft Matter* **2018**, *14*, 5098−5105.

(5) Zhang, Z.; Zhao, J.; Yan, X. Mechanically Interlocked Polymers with Dense Mechanical Bonds. *Acc. Chem. Res.* **2024**, *57*, 992−1006.

(6) Li, L.; Lin, Q.; Tang, M.; Tsai, E. H. R.; Ke, C. An Integrated Design of a Polypseudorotaxane-Based Sea Cucumber Mimic. *Angew. Chem. Int. Ed.* **2021**, *60*, 10186−10193.

(7) Du, R.; Xu, Z.; Zhu, C.; Jiang, Y.; Yan, H.; Wu, H. C.; Vardoulis, O.; Cai, Y.; Zhu, X.; Bao, Z.; Zhang, Q.; Jia, X. A Highly Stretchable and Self-Healing Supramolecular Elastomer Based on Sliding Crosslinks and Hydrogen Bonds. *Adv. Funct. Mater.* **2019**, *30*, No. 1907139.

(8) Feng, L.; Jia, S. S.; Chen, Y.; Liu, Y. Highly Elastic Slide-Ring Hydrogel with Good Recovery as Stretchable Supercapacitor. *Chem.—Eur. J.* **2020**, *26*, 14080−14084.

(9) Gao, R. M.; Yang, H.; Wang, C. Y.; Ye, H.; Cao, F. F.; Guo, Z. P. Fatigue-Resistant Interfacial Layer for Safe Lithium Metal Batteries. *Angew. Chem. Int. Ed.* **2021**, *60*, 25508−25513.

(10) Kato, K.; Nemoto, K.; Mayumi, K.; Yokoyama, H.; Ito, K. Ductile Glass of Polyrotaxane Toughened by Stretch-Induced Intramolecular Phase Separation. *ACS Appl. Mater. Interfaces* **2017**, *9*, 32436−32440.

(11) Murakami, T.; Schmidt, B. V. K. J.; Brown, H. R.; Hawker, C. J. One-Pot "Click" Fabrication of Slide-Ring Gels. *Macromolecules* **2015**, *48*, 7774−7781.

(12) Lin, Q.; Hou, X.; Ke, C. Ring Shuttling Controls Macroscopic Motion in a Three-Dimensional Printed Polyrotaxane Monolith. *Angew. Chem. Int. Ed.* **2017**, *56*, 4452−4457.

(13) Zhang, Y.; Chen, Y.; Li, J. Q.; Liu, S. E.; Liu, Y. Mechanical Stretch alpha-Cyclodextrin Pseudopolyrotaxane Elastomer with Reversible Phosphorescence Behavior. *Adv. Sci.* **2024**, *11*, No. e2307777.

(14) Bin Imran, A.; Esaki, K.; Gotoh, H.; Seki, T.; Ito, K.; Sakai, Y.; Takeoka, Y. Extremely stretchable thermosensitive hydrogels by introducing slide-ring polyrotaxane cross-linkers and ionic groups into the polymer network. *Nat. Commun.* **2014**, *5*, 5124.

(15) Jiang, L.; Liu, C.; Mayumi, K.; Kato, K.; Yokoyama, H.; Ito, K. Highly Stretchable and Instantly Recoverable Slide-Ring Gels Consisting of Enzymatically Synthesized Polyrotaxane with Low Host Coverage. *Chem. Mater.* **2018**, *30*, 5013−5019.

(16) Du, R.; Jin, Q.; Zhu, T.; Wang, C.; Li, S.; Li, Y.; Huang, X.; Jiang, Y.; Li, W.; Bao, T.; Cao, P.; Pan, L.; Chen, X.; Zhang, Q.; Jia, X. Sliding Cyclodextrin Molecules along Polymer Chains to Enhance the Stretchability of Conductive Composites. *Small* **2022**, *18*, No. e2200533.

(17) Lin, Q.; Ke, C. Conductive and anti-freezing hydrogels constructed by pseudo-slide-ring networks. *Chem. Commun.* **2021**, *58*, 250−253.

(18) Koyanagi, K.; Takashima, Y.; Yamaguchi, H.; Harada, A. Movable Cross-Linked Polymeric Materials from Bulk Polymerization of Reactive Polyrotaxane Cross-Linker with Acrylate Monomers. *Macromolecules* **2017**, *50*, 5695−5700.

(19) Yasuda, Y.; Hidaka, Y.; Mayumi, K.; Yamada, T.; Fujimoto, K.; Okazaki, S.; Yokoyama, H.; Ito, K. Molecular Dynamics of Polyrotaxane in Solution Investigated by Quasi-Elastic Neutron Scattering and Molecular Dynamics Simulation: Sliding Motion of Rings on Polymer. *J. Am. Chem. Soc.* **2019**, *141*, 9655−9663.

(20) Liu, C.; Morimoto, N.; Jiang, L.; Kawahara, S.; Noritomi, T.; Yokoyama, H.; Mayumi, K.; Ito, K. Tough hydrogels with rapid self-reinforcement. *Science* **2021**, *372*, 1078−1081.

(21) Jiang, Y.; Zhang, Z.; Wang, Y.-X.; Li, D.; Coen, C.-T.; Hwaun, E.; Chen, G.; Wu, H.-C.; Zhong, D.; Niu, S.; Wang, W.; Saberi, A.; Lai, J.-C.; Wu, Y.; Wang, Y.; Trotsyuk, A. A.; Loh, K. Y.; Shih, C.-C.; Xu, W.; Liang, K.; Zhang, K.; Bai, Y.; Gurusankar, G.; Hu, W.; Jia, W.; Cheng, Z.; Dauskardt, R. H.; Gurtner, G. C.; Tok, J. B.-H.; Deisseroth, K.; Soltesz, I.; Bao, Z. Topological supramolecular network enabled high-conductivity, stretchable organic bioelectronics. *Science* **2022**, *375*, 1411−1417.

(22) Tang, M.; Zheng, D.; Samanta, J.; Tsai, E. H. R.; Qiu, H.; Read, J. A.; Ke, C. Reinforced double-threaded slide-ring networks for accelerated hydrogel discovery and 3D printing. *Chem.* **2023**, *9*, 3515−3531.

(23) Wang, S.; Chen, Y.; Sun, Y.; Qin, Y.; Zhang, H.; Yu, X.; Liu, Y. Stretchable slide-ring supramolecular hydrogel for flexible electronic devices. *Commun. Mater.* **2022**, *3*, 2.

(24) Choi, S.; Kwon, T.-w.; Coskun, A.; Choi, J. W. Highly elastic binders integrating polyrotaxanes for silicon microparticle anodes in lithium ion batteries. *Science* **2017**, *357*, 279−283.
(25) Zhang, H.; Zhang, Y.; Chen, Y.; Wang, S.-P.; Zhang, C.; Liu, Y. Polyrotaxane in-situ copolymerization stretchable supramolecular hydrogels for photo-controlled cascade energy transfer. *Eur. Polym. J.* **2023**, *192*, No. 112070.
(26) Ma, S.; Lin, L.; Wang, Q.; Zhang, Y.; Zhang, H.; Gao, Y.; Xu, L.; Pan, F.; Zhang, Y. Modification of Supramolecular Membranes with 3D Hydrophilic Slide-Rings for the Improvement of Antifouling Properties and Effective Separation. *ACS Appl. Mater. Interfaces* **2019**, *11*, 28527−28537.
(27) Xia, H.; Xu, G.; Cao, X.; Miao, C.; Zhang, H.; Chen, P.; Zhou, Y.; Zhang, W.; Sun, Z. Single-Ion-Conducting Hydrogel Electrolytes Based on Slide-Ring Pseudo-Polyrotaxane for Ultralong-Cycling Flexible Zinc-Ion Batteries. *Adv. Mater.* **2023**, *35*, No. e2301996.
(28) Xiong, X.; Chen, Y.; Wang, Z.; Liu, H.; Le, M.; Lin, C.; Wu, G.; Wang, L.; Shi, X.; Jia, Y. G.; Zhao, Y. Polymerizable rotaxane hydrogels for three-dimensional printing fabrication of wearable sensors. *Nat. Commun.* **2023**, *14*, 1331.
(29) Choi, D.; Lee, Y.; Lin, Z. H.; Cho, S.; Kim, M.; Ao, C. K.; Soh, S.; Sohn, C.; Jeong, C. K.; Lee, J.; Lee, M.; Lee, S.; Ryu, J.; Parashar, P.; Cho, Y.; Ahn, J.; Kim, I. D.; Jiang, F.; Lee, P. S.; Khandelwal, G.; Kim, S. J.; Kim, H. S.; Song, H. C.; Kim, M.; Nah, J.; Kim, W.; Menge, H. G.; Park, Y. T.; Xu, W.; Hao, J.; Park, H.; Lee, J. H.; Lee, D. M.; Kim, S. W.; Park, J. Y.; Zhang, H.; Zi, Y.; Guo, R.; Cheng, J.; Yang, Z.; Xie, Y.; Lee, S.; Chung, J.; Oh, I. K.; Kim, J. S.; Cheng, T.; Gao, Q.; Cheng, G.; Gu, G.; Shim, M.; Jung, J.; Yun, C.; Zhang, C.; Liu, G.; Chen, Y.; Kim, S.; Chen, X.; Hu, J.; Pu, X.; Guo, Z. H.; Wang, X.; Chen, J.; Xiao, X.; Xie, X.; Jarin, M.; Zhang, H.; Lai, Y. C.; He, T.; Kim, H.; Park, I.; Ahn, J.; Huynh, N. D.; Yang, Y.; Wang, Z. L.; Baik, J. M.; Choi, D. Recent Advances in Triboelectric Nanogenerators: From Technological Progress to Commercial Applications. *ACS Nano* **2023**, *17*, 11087−11219.
(30) Li, R.; Xu, Z.; Li, L.; Wei, J.; Wang, W.; Yan, Z.; Chen, T. Breakage-resistant hydrogel electrode enables ultrahigh mechanical reliability for triboelectric nanogenerators. *Chem. Eng. J.* **2023**, *454*, No. 140261.
(31) Liu, T.; Liu, M.; Dou, S.; Sun, J.; Cong, Z.; Jiang, C.; Du, C.; Pu, X.; Hu, W.; Wang, Z. L. Triboelectric-Nanogenerator-Based Soft Energy-Harvesting Skin Enabled by Toughly Bonded Elastomer/Hydrogel Hybrids. *ACS Nano* **2018**, *12*, 2818−2826.
(32) Wang, Y.; Zhang, L.; Lu, A. Highly stretchable, transparent cellulose/PVA composite hydrogel for multiple sensing and triboelectric nanogenerators. *J. Mater. Chem. A* **2020**, *8*, 13935−13941.
(33) Wen, Z.; Yang, Y.; Sun, N.; Li, G.; Liu, Y.; Chen, C.; Shi, J.; Xie, L.; Jiang, H.; Bao, D.; Zhuo, Q.; Sun, X. A Wrinkled PEDOT:PSS Film Based Stretchable and Transparent Triboelectric Nanogenerator for Wearable Energy Harvesters and Active Motion Sensors. *Adv. Funct. Mater.* **2018**, *28*, No. 1803684.
(34) Zhu, R.; Zhu, D.; Zheng, Z.; Wang, X. Tough double network hydrogels with rapid self-reinforcement and low hysteresis based on highly entangled networks. *Nat. Commun.* **2024**, *15*, 1344.

https://doi.org/10.1021/acsami.4c12962
ACS Appl. Mater. Interfaces 2024, 16, 68229−68236